Pergamon

Cement and Concrete Research 31 (2001) 1043–1048

CEMENT AND CONCRETE RESEARCH

Estimating the cut-off in the fractal scaling of fractured concrete

L.T. Dougan*, P.S. Addison

Civil Engineering Group, School of the Built Environment, Napier University, Merchiston Campus, 10 Colinton Road, Edinburgh, EH10 5DT, Scotland, UK

Received 31 October 2000; accepted 2 April 2001

Abstract

An experimental study of the fractal scaling of concrete fracture is described. A concrete beam subjected to three-point bending in flexure was loaded to failure and the fracture surface viewed at various magnifications using a scanning electron microscope (SEM). The fractal dimension was then computed for 50 samples using the variable bandwidth technique. The results indicate that the fractal dimension tends towards unity at high magnification, indicating a return to Euclidean form. This suggests that the crack surface has a cut-off in fractal scaling in the region 0.63 to 4.57 nm. © 2001 Elsevier Science Ltd. All rights reserved.

Keywords: SEM; Microstructure; Calcium silicate hydrate (C-S-H)

1. Introduction

The development of analytical models to describe the fractal behaviour of fracture within a material has been driven by the desire to explain cracking phenomena and to quantify material parameters. Several studies have shown that concrete cracks can be characterised by fractals [1–8] and others have adopted fractals to quantify fracture behaviour [9–22]. Very little is known about concrete at small scales. Jennings [23] stated that calcium silicate hydrate (C-S-H), the bonding gel between aggregates "has not been modelled precisely" between 1 and 100 nm. Recently, Addison [22] formulated a prefractal model to evaluate fracture energy for self-affine crack surfaces that have a Euclidean cut-off at small scales. This model allows for a prefractal or a true area to be computed with normal units of area. The prefractal model has a distinct advantage over other fractal models as it produces the same size effect law as incorporated by recent fractal theories, while retaining the correct physical dimensions. This study identifies the scale at which a concrete crack stops behaving as a fractal and acts as a Euclidean entity. At this point, a true finite area can be found. This can then be readily determined and used to evaluate accurately the fracture energy and hence, the fracture toughness of the material.

This paper describes recent work by the authors in determining a prefractal cut-off region for cracked concrete specimens. The rest of the paper is structured as follows: in Section 2, a brief account is given of the techniques employed in obtaining crack data; Section 3 contains a description of the fractal analysis undertaken; results of the study are presented in the Section 4; and a discussion of the results is given in Section 5.

2. Data acquisition

The data used for the study came from a single concrete beam similar to those used in previous studies [1]. The beam was 40-mm wide, 30-mm deep and 300-mm long, it was loaded in a three-point bending test after 28 days. After failure, one of the fractured surfaces was removed for the analysis. The crack surface under investigation came from the tension face of the beam, i.e., the face from which the crack propagates (see Fig. 1). The concrete consisted of ordinary Portland Cement and a well graded crushed rock aggregate with a maximum size of 10 mm that complied with grading envelopes as given in BS882: 1983. The concrete mix had a water/cement ratio of 0.55:1.0 and was designed to have a characteristic strength of 30 N/mm^2 after 28 days.

A scanning electron microscope (SEM) was used to examine the crack surfaces and acquire image data for analysis. This instrument offers two distinct advantages over optical microscopes: very high resolutions and a

* Corresponding author. Tel.: +44-131-455-2685; fax: +44-131-455-2239.

E-mail address: l.dougan@napier.ac.uk (L.T. Dougan).

PII: S0008-8846(01)00518-X

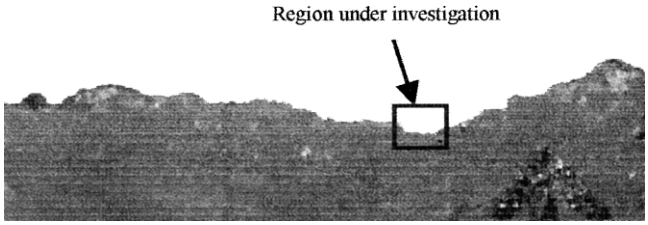

Fig. 1. Sample, 40 mm across at the widest part, showing area of SEM inspection.

large depth of field. This allows for a comprehensive study of the concrete microstructure through a range of scales. Several previous studies of the microstructure of concrete have employed the SEM [24–27]. The specimen was examined at magnifications varying from 35× to 385,000× corresponding to image lengths of 6 mm to 560 nm, respectively. Fig. 2 contains a selection of typical images. The crack was viewed on the microscope's screen and images were downloaded to an attached computer and saved as image files. The images all came from a region covering approximately 5 mm of the crack as indicated by the box in Fig. 1. The crack was first viewed at a magnification of approximately 35×. The magnification was then increased in stages up to 385,000× (see Fig. 2). To separate the crack image edge from the rest of the image, the saved files were then filtered to remove any unwanted information. This filtering process is described elsewhere [1]. Once the crack edge had been isolated, an in-house computer program was then used to abstract the crack edge as a series of pixel coordinates.

A remarkable new result in fractal analysis [28] has shown that the horizon or silhouette of a surface should possess the same fractal dimension as a section through the surface (i.e., its profile). This allows us, for the first time, to use SEM images to estimate the fractal dimension of surfaces through the well known relationship between the dimension of the surface and its corresponding profile. This simply states that the $D_{f(surface)} = D_{f(profile)} + 1$.

3. Fractal analysis

The fractal dimension of each image was computed using the variable bandwidth technique [1–4]. This method interrogates the crack along its length using a variable width window of a specified length S. The window slides along the crack at a specific value of S and the displacement, ΔB, is calculated for each window

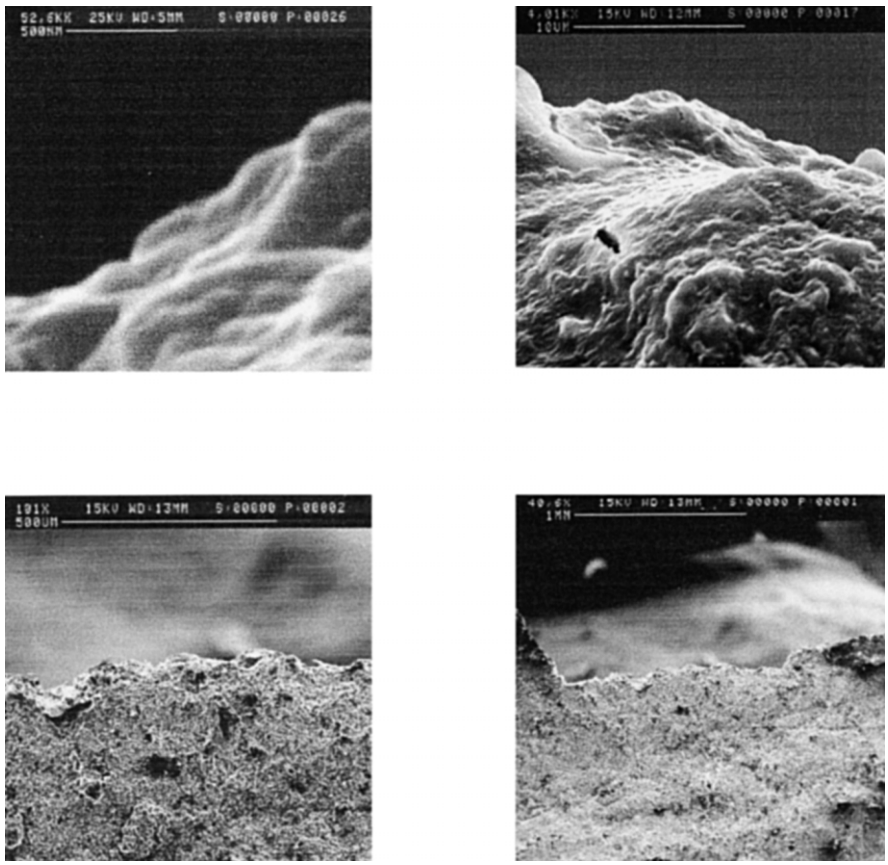

Fig. 2. SEM images of the crack profiles at (top left) 52,600×, (top right) 4010×, (bottom left) 101× and (bottom right) 40×.

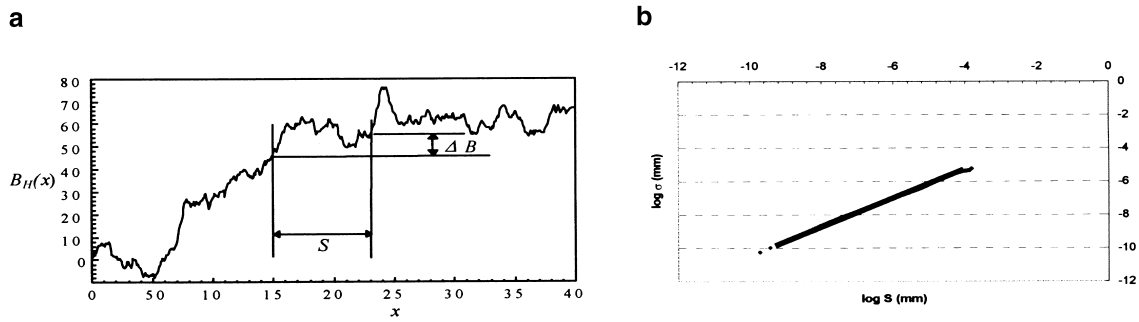

Fig. 3. The variable bandwidth method. a) A window of length S is ran over the data and the excursion ΔB is computed at each location b) The standard deviation of the excursion against window length S gives H and K_f(4,010×).

position (see Fig. 3a). The standard deviation of the displacements, σ_s, are calculated for a range of window sizes as follows (Eq. (1)):

$$\sigma_s = \sqrt{\frac{1}{N-\mathrm{NS}} \sum_{i=1}^{N-\mathrm{NS}} (\Delta B)^2} \quad (1)$$

where N is equal to the total number of data points and NS is equal to the number of data points corresponding to the sliding window. For a random fractal fracture exhibiting fractional Brownian type behaviour [1–5,29–32], we expect σ_s to scale as (Eq. (2)):

$$\sigma_s = \sqrt{2K_f} S^H \quad (2)$$

where K_f is a diffusion-type coefficient and H is the Hurst exponent. A bilogarithmic plot of standard deviation vs. window size is used to determine these parameters (Fig. 3b). The slope of the plot gives H, which can be used to describe the roughness of the crack. The Hurst coefficient is related to the fractal dimension of the crack trace through the simple relationship $D_f = 2 - H$. The K_f value can be determined using the point where the best-fit line crosses the log(σ) axis [1–4]. The variable bandwidth technique was used because it has been proven to give accurate results for fracture data [3], as well as leading directly to the spatial diffusion coefficient K_f [1]. Another commonly used method for computing fractal dimension is the box counting technique [3,4,8,12,15,19], which gives results of a similar accuracy, but does not give K_f. Other popular techniques include spectral analysis using either Fourier or wavelet transforms. However, previous studies by the authors and others have found that these methods are not accurate for self-affine profiles unless ensemble averaging is employed on a large number of data sets [3,33].

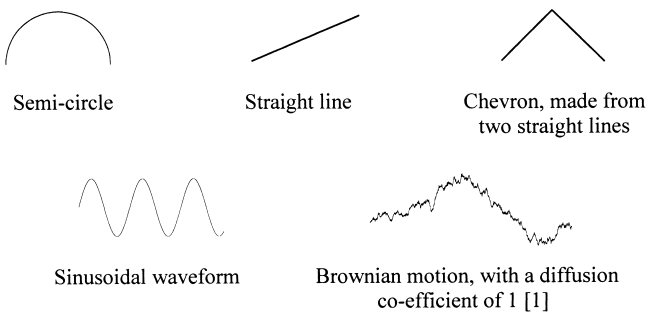

Fig. 4. Test data for variable bandwidth method, each shape or trace contains 1024 points.

4. Results

The variable bandwidth technique used in the fractal analysis was checked using five simple test objects with known fractal dimensions: a semicircle; a straight line; a chevron; a sinusoidal waveform (all with dimension 1) and a Brownian motion trace with a fractal dimension of 1.5. They are shown in Fig. 4. The analysis produced dimensions that gave a maximum error of ±3.2% (Table 1). In a previous study by the authors [3], the fractal dimension of synthesised fractional Brownian traces were computed using several methods. In this previous study, the variable bandwidth technique proved to be one of the two most accurate methods for determining the fractal dimension (the other being the box counting method). However, the variable bandwidth method was considered preferable as it also provides an estimate of the spatial diffusion coefficient, K_f, in addition to the fractal dimension.

Fig. 5 shows both the Hurst coefficient, H and the corresponding fractal dimension, D_f ($=2-H$) of the crack traces against magnification for each of the 50 images analysed. From this plot, it can be seen that the results fit into an envelope (the shaded area in Fig. 5) that gradually collapses towards unity at high magnification. Fig. 6 shows the spreading of the results in relation to scale. Notice that it shows a sudden decrease in the fractal dimension at

Table 1
Results from testing method

Objects	Fractal dimension
Semicircle	1.032
Straight line	1.020
Chevron	1.016
Waveform	1.026
Brownian trace	1.453

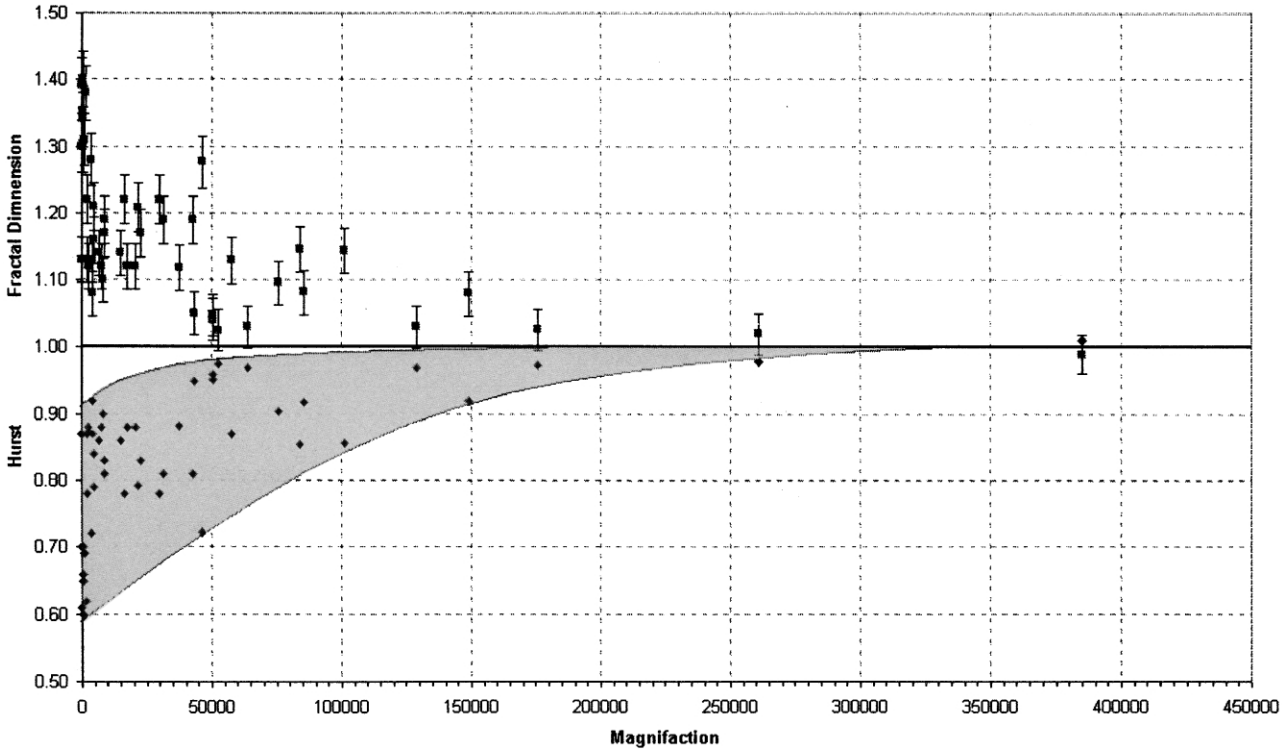

Fig. 5. Plot showing both the Hurst exponent and fractal dimension against magnification for all 50 cracks. 3.2% error bars are shown on the fractal dimension data.

approximately 5 nm. The values at scales larger than 5 nm compare favourably to those values stated at similar scales in other studies [1–8]. However, the fractal dimension estimates at scales less than 5 nm drop rapidly to values

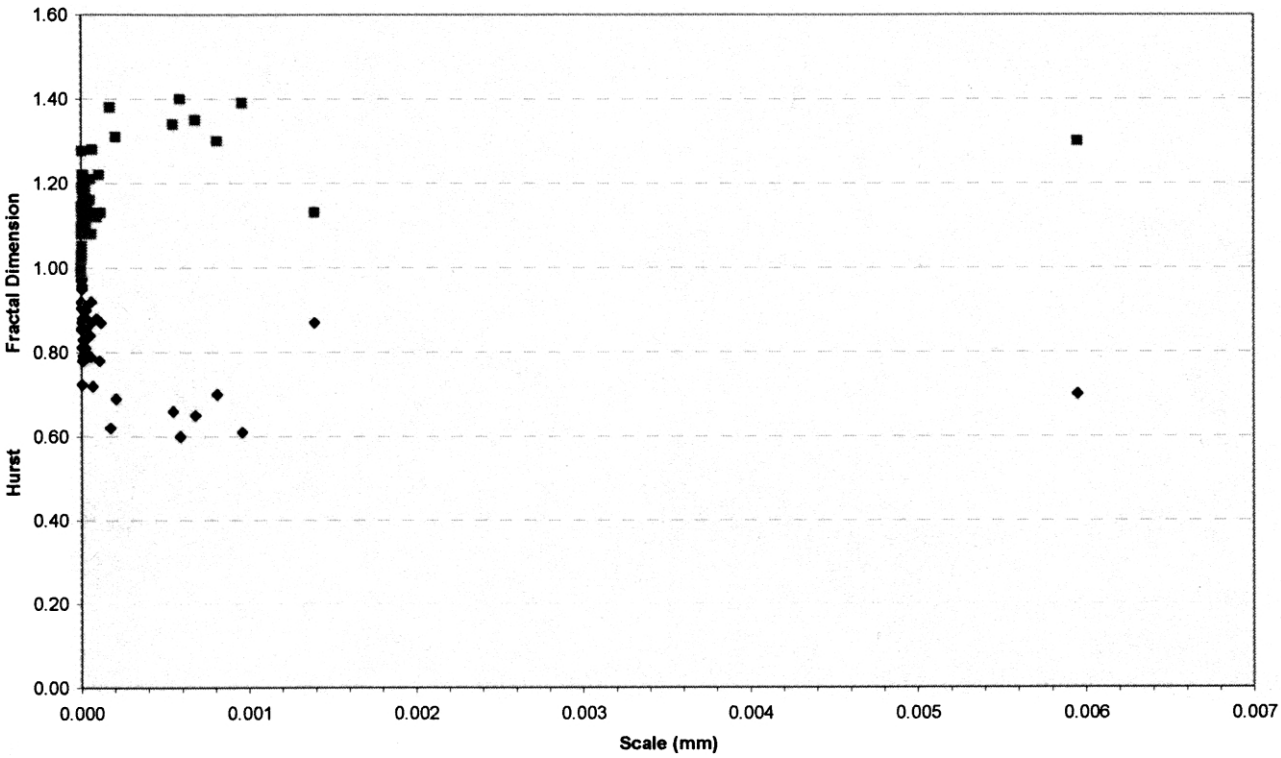

Fig. 6. Scale vs. the Hurst coefficient and fractal dimension.

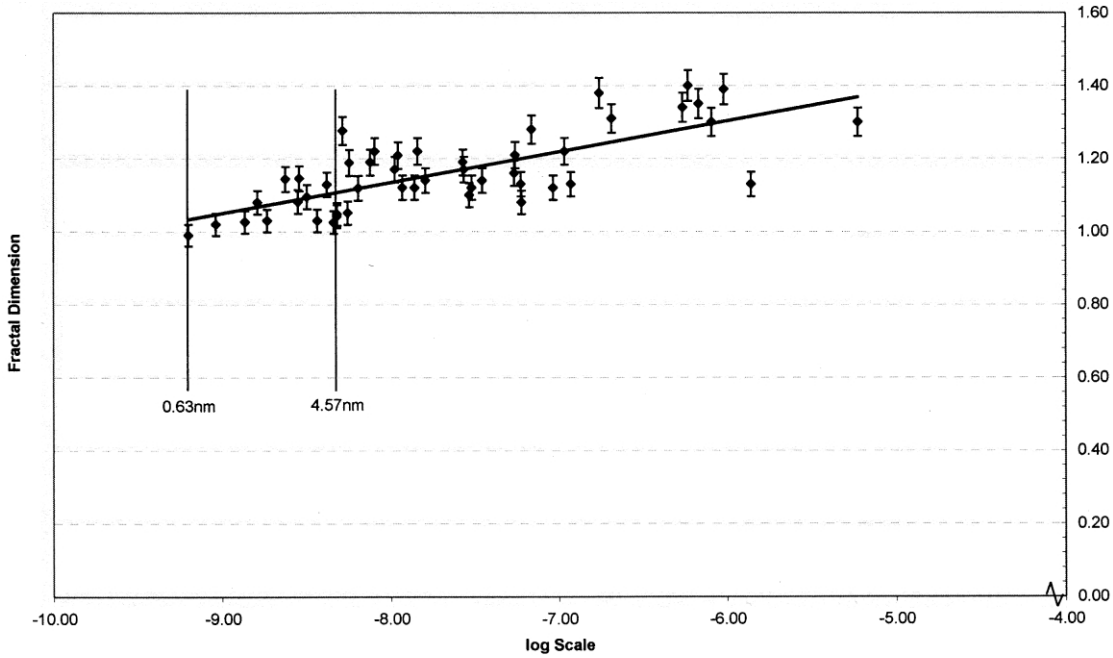

Fig. 7. Logarithmic plot of scale vs. dimension with 3.2% error bars shown.

close to unity, indicating that the crack is rapidly becoming Euclidean in nature in this region. This plot was derived from the data in Fig. 5 as the scale for each image varies according to magnification and working distance, therefore a scale could be calculated individually for each trace. A value of millimeters (mm) per pixel was calculated from the scale given on each image (see Fig. 2). The minimum window size used in the variable bandwidth method was set at three pixels. Hence, the minimum physical scale for each image, $S_{\min}$, could be computed. This lower-bound scale was then set as the scale in Fig. 5. Fig. 7 contains a semilogarithmic plot of the fractal dimension plotted against scale. Two vertical lines are present in the plot. These lines represent the region where, within a 3.2% error bound, a fractal dimension of 1 is found. The upper-bound value of this region equates to a scale of 4.57 nm and a lower-bound value of 0.63 nm. A best-fit line has also been placed on the plot showing the general trend of results. This best-fit line is given by:

$$D_{\mathrm{f}} = 0.081\log(S_{\min}) + 1.81 \qquad (3)$$

5. Concluding remarks

The work described above has attempted to identify the cut-off in the fractal description of a concrete crack surface. The results show that, with increasing magnification, the fractal dimension tends towards unity, reaching unity at between 0.63 and 4.57 nm, at which point the crack becomes Euclidean in form. These boundaries of 0.63 and 4.57 nm correspond to the range we would expect C-S-H to fall into [23,34]. "Various studies have indicated structural relationships to tobermorite, especially in its 1.4 nm form ($C_5S_6H_9$), or jennite ($C_9S_6H_{11}$)," as stated by Taylor [35]; such small elements have been related to fractals and referred to as monomers by Feder [36]. Saouma and Barton [19] previously considered C-S-H to base a minimum fractal scale on, however, they estimated the scale to be approximately 10 μm.

The main results from this study are given in Fig. 7 where a clear trend in the reduction of fractal dimension with decreasing scale is evident. We have defined this trend by Eq. (3), although, at present, we have no physical explanation of the exact form of this trend. It is expected that the prefractal cut-off scale will not change significantly for other concrete mixes, as previous studies investigating different concretes have found similar fractal dimensions for fracture surfaces. Further work by the authors will attempt to verify this. In addition, future work will look for a physical explanation of the reduction in dimension with decreasing scales. In addition, the relationship between the fractal dimension, and its associated cut-off scale, and the concrete mix will be investigated.

Acknowledgments

The authors would like to thank Bill Brownlee for his assistance in obtaining data for analysis.

References

[1] P.S. Addison, W.M.C. McKenzie, A.S. Ndumu, L.T. Dougan, R. Hunter, Fractal cracking of concrete: Parameterisation of spatial diffusion, ASCE J. Eng. Mech. 125 (6) (1999) 622–629.

[2] P.S. Addison, W.M.C. McKenzie, L.T. Dougan, A.S. Ndumu, A Complete Geometric Description of Cracked Concrete, In: N.P. Jones, R.G. Ghanem, (Eds.), 13th ASCE Engineering Mechanics Division Conference, The John Hopkins University, Baltimore, on CR-ROM, 1999. Baltimore, MD, USA, 1999 (June 13–16).
[3] L.T. Dougan, P.S. Addison, Fractal analysis of fracture: A comparison of dimension estimates, Mech. Res. Commun. 27 (4) (2000) 383–392.
[4] P.S. Addison, Fractals and Chaos: An Illustrated Course, Institute of Physics Publishing, London, 1997.
[5] A.M. Hammad, M.A. Issa, Fractal dimension as a measure of roughness of concrete fracture trajectories, Adv. Cem. Based Mater. 1 (1994) 169–177.
[6] M.A. Issa, A.M. Hammad, Fractal characterisation of fracture surfaces in mortar, Cem. Concr. Res. 23 (1993) 7–12.
[7] M.A. Issa, A.M. Hammad, Assessment and evaluation of fractal dimension of concrete fracture surface digitised images, Cem. Concr. Res. 24 (2) (1994) 325–334.
[8] V.E. Saouma, C.C. Barton, N.A. Gamaleldin, Fractal characterisation of fracture surfaces in concrete, Eng. Fract. Mech. 35 (1990) 47–53.
[9] Z.P. Bazant, E. Chen, Scaling of structural failure, ASME Appl. Mech. Rev. 50 (1997) 593–627.
[10] Z.P. Bazant, Scaling of quasi-brittle fracture and the fractal question, J. Eng. Mater. Technol. 117 (1995) 361–367.
[11] J.P. Bouchaud, E. Bouchaud, G. Lapasset, J. Planès, Models of fractal cracks, Phys. Rev. Lett. 71 (14) (1993) 2240–2243.
[12] F.M. Borodich, Some fractal models of fracture, J. Mech. Phys. Solids 45 (2) (1997) 239–259.
[13] A. Carpinteri, Scaling laws and renormalization groups for strength and toughness of disordered materials, Int. J. Solids Struct. 31 (3) (1994) 291–302.
[14] A. Carpinteri, G. Ferro, Size effects on tensile fracture properties: A unified explanation based on disorder and fractality of concrete microstructure, Mater. Struct. 27 (1994) 563–571.
[15] A. Carpinteri, B. Chiaia, S. Invernizzi, Three-dimensional fractal analysis of concrete fracture at the meso-level, Theor. Appl. Fract. Mech. 31 (3) (1999) 163–172.
[16] B. Chiaia, J.G.M. van Mier, A. Vervuurt, Crack growth mechanisms in four different concretes: Microscopic observations and fractal analysis, Cem. Concr. Res. 28 (1) (1998) 103–114.
[17] J. Peng, Z. Wu, G. Zhao, Fractal analysis of fracture in concrete, Theor. Appl. Fract. Mech. 27 (1997) 135–140.
[18] A.B. Mosolov, Mechanics of fractal cracks in brittle solids, Europhys. Lett. 24 (8) (1993) 643–678.
[19] V.E. Saouma, C.C. Barton, Fractals, fractures, and size effects in concrete, ASCE J. Eng. Mech. 120 (4) (1994) 835–854.
[20] H. Xie, Effects of fractal crack, Theor. Appl. Fract. Mech. 23 (3) (1995) 235–244.
[21] X.H. Ji, S.Y.N. Chan, N.Q. Feng, A fractal model for simulating the formation of microcracks in the fracture process zone and a theoretical explanation of the size effect of the fracture energy of concrete, Mag. Concr. Res. 49 (180) (1997) 253–258.
[22] P.S. Addison, The geometry of prefractal renormalisation: Application to crack surface energies, Fractals 8 (2) (2000) 147–153.
[23] H.M. Jennings, A model for the microstructure of calcium silicate hydrate in cement paste, Cem. Concr. Res. 30 (2000) 101–116.
[24] A. Carpinteri, B. Chiaia, K.M. Nemati, Complex fracture energy dissipation in concrete under different loading conditions, Mech. Mater. 26 (2) (1997) 93–108.
[25] K.O. Kjellsen, M.H. Jennings, Observations of microcracking in cement paste upon drying and rewetting by environmental scanning electron microscopy, Adv. Cem. Based Mater. 3 (1996) 14–19.
[26] K.M. Nemati, Fracture analysis of concrete using scanning electron microscopy, Scanning 19 (6) (1997) 426–430.
[27] S. Diamond, Aspects of concrete porosity revisited, Cem. Concr. Res. 29 (1999) 1181–1188.
[28] K.J. Falconer, J. Lévy Véhel, Horizons of fractional Brownian surfaces, Proc. R. Soc., London, Ser. A 456 (2000) 2153–2177.
[29] A. Chudnovsky, B. Kunin, A probabilistic model of brittle crack formation, J. Appl. Phys. 62 (10) (1987) 4124–4129.
[30] B. Kunin, M. Gorelik, On representation of fracture profiles by fractional integrals of a Weiner process, J. Appl. Phys. 70 (12) (1991) 7651–7653.
[31] H.O. Peitgen, D. Saupe (Eds.), The Science of Fractal Images, Springer-Verlag, New York, 1998.
[32] Z.-M. Yin, New methods for simulation of fractional Brownian motion, J. Comp. Phys. 127 (1996) 66–72.
[33] J. Schmittbuhl, S. Roux, Y. Berthaud, Development of roughness in crack propagation, Europhys. Lett. 28 (8) (1994) 585–590.
[34] I.G. Richardson, The nature of C-S-H in hardened cements, Cem. Concr. Res. 29 (1999) 1131–1147.
[35] H.F.W. Taylor, Nanostructure of C-S-H: Current status, Adv. Cem. Based Mater. 1 (1993) 38–46.
[36] J. Feder, Fractals, Plenum, New York, NY, 1988.